Faculty of Geo-sciences
MSc Program Earth Surface and Water

MSc Graduation Research

Automated Identification and Analysis of Ice Keel Scours in the Beaufort Sea: Insights into Sea Ice and Seabed Interactions through Bathymetric Data Analysis

Author: Nikolaos Kallioras

Utrecht University First Supervisor: Dr. ir. Jaap Nienhuis
Utrecht University Second Supervisor: Dr. Menno Straatsma

April 13, 2024

Abstract

This geoscience thesis focuses on the automated identification and analysis of ice keel scours in Harrison Bay, part of the Beaufort Sea. The study area includes the Colville River Delta and is stationed close to oil and gas exploration and shipping activities. The study utilizes bathymetric data acquired from multibeam surveys with advanced automated feature extraction techniques. This includes the Modified Multiscale Singularity Index to identify and analyze ice keel scours. The algorithm developed processed a dataset spanning 45 square kilometers and successfully extracted crucial metrics that are comparable to those obtained in prior research studies. The study's findings suggest that ice keel scours are a critical mechanism of sediment transport in Harrison Bay and may have implications for the design and operation of offshore structures and pipelines. Results from this study show that the most common scour width interval was between 1.0 and 3.0 meters. The density of scours was observed to increase linearly with depth. The orientation of the measured scours aligned with the prevailing sea ice movements in the region, indicating a south-eastern direction (100°). The study provides insights into sediment transport dynamics and ice sheet movement in the Beaufort Sea. It highlights the potential for further research and improvements in automated identification and analysis techniques, including developing more accurate and efficient algorithms for identifying and analyzing the scours.

Table of Contents

List of Figures

1 Introduction

Ice keel scours are the result of floating ice features that drift into shallow areas and interact with the seabed (Reimnitz et al., 1978). These features are typically icebergs and sea ice ridges and highlight the dynamic interaction between ice and the seafloor. The process of ice scouring intensifies the bottom sediment transport by enhancing the near-bottom currents with the movement of the ice keels (Barnes et al., 1987). Furthermore, ice dynamics, including the movement and deformation of ice, significantly influence ice scouring density. Investigating these scours found on the seafloor can offer critical insights into the underlying ice dynamics.

Despite significant advancements in ice dynamics research, including data acquisition and computational analysis capabilities, the study of ice keel scours has yet to incorporate these improved methods fully. Technologies such as sonar-based bathymetric mapping have made significant advancements, resulting in a wealth of new and detailed data grids as demonstrated by the groundbreaking work of Weatherall et al., 2015 and recent studies like Szafarczyk and Toś, 2022. In the past, researchers were limited to using pre-existing software for data analysis. However, recent advancements in autonomous techniques, particularly in image processing, offer promising alternatives for analyzing vast amounts of data. This is demonstrated in the study by Nellikkattil et al., 2024, which focuses on climate data. Utilizing advanced feature extraction methods is essential in enhancing the accuracy and efficiency of identifying, mapping, and analyzing features. With automated extraction of ice keel scours, researchers can analyze large datasets more efficiently, uncover subtle patterns and changes over time, and gain deeper insights into the underlying dynamics. However, the application of such automation to analyze ice keel scours still needs to be improved, highlighting a gap in applying modern methodologies to this specific area of ice dynamics research.

The singularity index (SI) is a powerful technique that can extract critical features from complex data, regardless of its form or dimension (Muralidhar et al., 2012). Specifically, the Singularity index, utilizes Gaussian derivatives to accurately identify curvilinear patterns while filtering out irrelevant information. This technique can be utilized to develop highly targeted and efficient feature extraction frameworks, as demonstrated in the RivaMap engine by Isikdogan et al., 2017. Isikdogan et al., 2017 adapted the multiscale singularity index for fully automated extraction on river networks, showcasing the versatility of this approach, which suggests its potential usefulness in extracting ice keel scours features.

The Beaufort Sea, located north of Alaska, presents an ideal location for automated ice keel scour analysis. According to estimates from the mid-2010s, sea ice coverage persists for approximately nine months each year in this region (Wang and Overland, 2015), making it a critical area for comprehending the interactions between sea ice and the seafloor. Furthermore, this region is significant in offshore oil and gas exploration, making the challenges of ice gouging essential to address. By analyzing scour patterns in specific areas, we can obtain vital information on the integrity of sub-sea pipelines, which are crucial for resource transportation (Hill et al., 1991). Due to the Beaufort Sea's unique characteristics, several studies have been conducted. Reimnitz et al., 1978 delved into the complex composition of sea ice and the geological shaping caused by ice keel scouring, focusing on the stamukhi zone. However, these findings are based on studies that have been around for more than three decades. Given the dynamic nature of the Arctic environment and the significant changes ice canopies are expected to undergo due to climate change (Wang and Overland, 2015), there is an urgent need to reassess our understanding of these processes.

This thesis aims to develop a methodology for detecting and analyzing ice keel scours automatically, using high-resolution bathymetry data. By analyzing the patterns of keel scours in the Beaufort Sea, this study aims to improve our understanding of ice dynamics and their impact on seabed morphology. It is based on the hypothesis that keel scour patterns are crucial indicators of the interactions between sea ice and the seabed.

2 Literature Research

2.1 Sea Ice

2.1.1 Sea Ice seasonality

According to Shokr and Sinha, 2023, sea ice is crucial to the Earth's climate system. The importance of sea ice is seen in the extent to which sea ice covers the ocean surface, which is between 7% and 15%, depending on the season. In the Arctic, the sea ice starts forming in September and reaches its peak in March, when it covers the entire Arctic basin. The trend is reversed during the summer, and the ice extent reaches its minimum in September. This annual cycle of sea ice production and degradation is vital in regulating the world's climate and significantly impacts oceanic processes down to the abyss (Dieckmann, 2003).

2.1.2 Sea Ice Movement

Research has shown that wind and ocean currents are the primary influencers of sea ice movement. The Beaufort Sea Gyre (BSG) is shown in Figure 1 and recognized as a significant factor in the movement of sea ice along Alaska's continental margin, according to studies conducted by Eicken et al., 2005 and Reimnitz et al., 1978. Increased sea ice movement also results in increased thickness as a result of mechanical collisions. The study of sea ice mobility is critical in understanding how it affects ice shelf morphology and sediment transport. Additionally, analyzing seabed and ice keel scours can provide insights into the direction of sea ice movement.

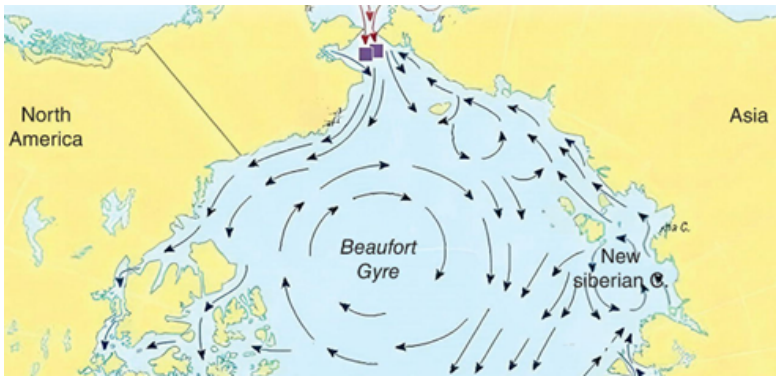

Figure 1: Map illustrating the circulation of the Beaufort Gyre in the Arctic Ocean between North America and Asia. [Image from National Snow and Ice Data Center / Arctic Monitoring and Assessment Programme, 2021].

2.1.3 Sea Ice Thickness

Sea ice primarily grows through thermodynamic processes that occur due to the temperature difference between the atmosphere and seawater. This causes thin ice to grow faster than thicker ice, resulting in horizontal rather than vertical growth. However, as mentioned before sea ice can also thicken mechanically when it converges and collides. This is called sea ice deformation and can lead to three primary types of features:

1. Rafted ice, where one piece of ice overrides another.
2. Hummocks, which are mounds of broken ice that create an uneven surface.
3. Pressure ridges shown in Figure 2, which are lines of broken ice forming a ridge that extends above the sea level, referred to as a sail, and a part that extends under the freeboard forming a keel.

These pressure ridges are responsible for the ice keel scours formed from sea ice and hold Between 30 to 80 percent of the ice volume in an ice field (Thomas, 2017). As a result, studying these pressure ridges is of great importance for scientists to enhance their understanding of sea ice dynamics and its impact on the surrounding environment.

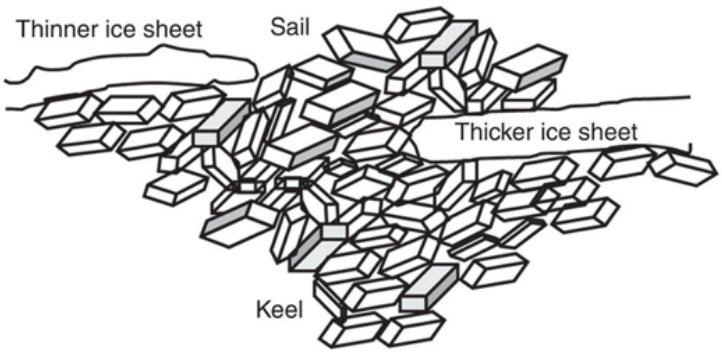

Figure 2: Sketch of a Pressure Ridge formed by the collision of thinner and thicker ice sheets. Blocks break off the sheets and form the sail and the keel. [Image from Shokr and Sinha, 2023].

2.2 Sea Ice Zones

2.2.1 Sea Ice Zone Classification

Sea ice is classified based on its attachment to the shore. Ice frozen or attached to the shoreline is known as landfast ice or fast ice. On the other hand, drift ice or pack ice is found further offshore and covers vast areas (Shokr and Sinha, 2023). It is not anchored to the shoreline and can move freely under the influence of winds and currents. Drift ice undergoes complex deformation processes due to the interactions between moving ice floes.

2.2.2 Stamukhi Zone Characteristics

At the boundary between fast ice and drifting pack ice, where the collision of sea ice is prominent, grounded accumulations of sea ice rubble called stamukhi are formed. The accumulations are typically pressure ridges that can last several years safeguarding shores from ice pressure and resembling islands in their effect. These accumulations can be seen in Figure 3 where they typically align parallel to the coastline and form what is known as the stamukhi zone. The stamukhi zone can be found in shallow Arctic regions, at depths around 20m, potentially reaching 50m (Barnes et al., 1987). This zone influences sediment distribution on the shelf due to the intense early winter ridge grounding and seabed scouring. This results in the creation of ice keel scours studied in this thesis.

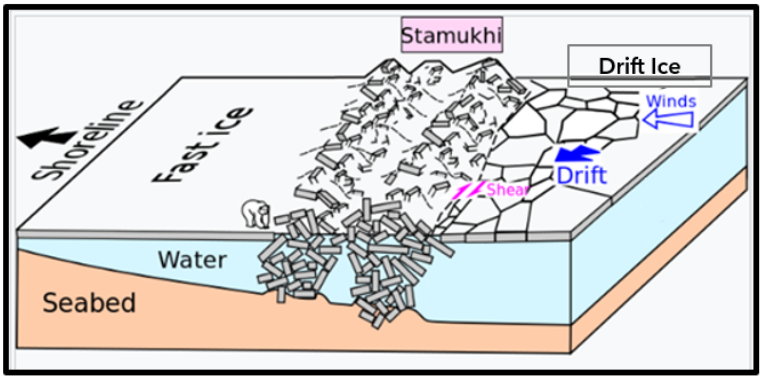

Figure 3: Sketch illustrating the sea ice zones, with the stamukhi located between the Fastened and the Drift pack ice zones. [Original image from Lusilier, 2023b]

2.3 Ice Keel Scours

As mentioned before Ice Keel Scours are formed when the keels of floating ice features such as icebergs or pressure ridges come into contact with the seabed. This interaction creates linear scours or gouges in the seafloor along with two parallel ridges of displaced sediment, as schematically shown in Figure 4. These scours can span several kilometers and occur at varying depths, from a few meters to hundreds of meters.

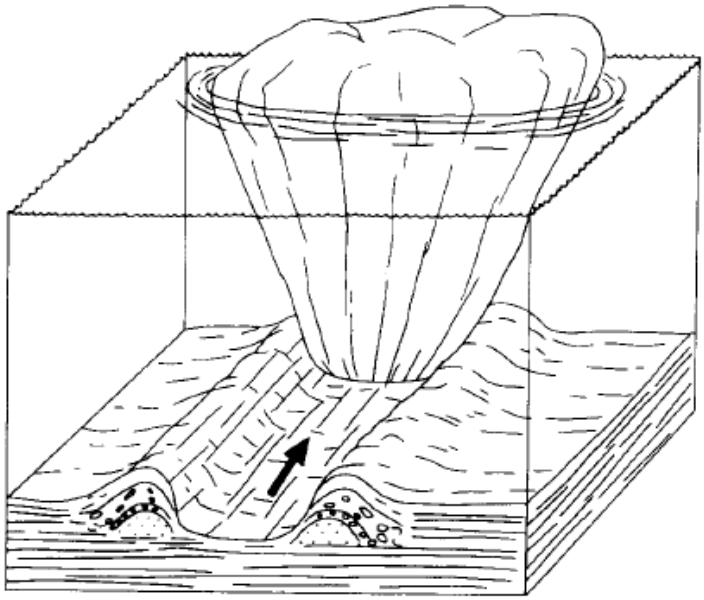

Figure 4: Sketch of an iceberg keel plowing through the seabed and creating two parallel ridges. [Original image from Zhang, 1992].

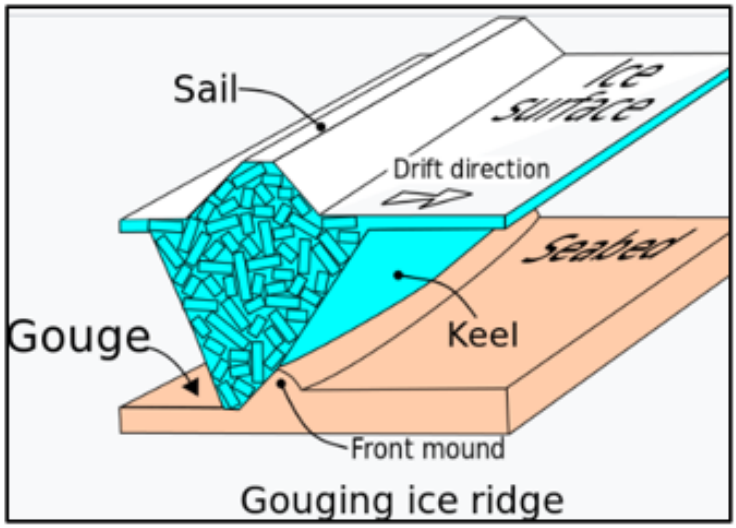

Figure 5: Sketch of a pressure ridge forming a keel scour with only one parallel side ridge. [Original image from Lusilier, 2023a]

The characteristics of these scour phenomena can differ greatly. Studies by Héquette et al., 1995 have revealed that most scours in the Arctic have a depth of less than 60 centimeters, while Blasco et al., 1998 identified a scour measuring 8.5 meters in depth at depths ranging from 40 to 50 meters. Similarly, the width of scours can vary considerably, with most scours ranging from 2 to 8 meters in width, but some measuring over 40 meters. Ice keel scours from icebergs and sea ice ridges are also different. Scours from icebergs are generally at lower depths and show deeper gouges than sea ice ridges that form in shallower waters. Scours formed by sea ice are mainly done from pressure ridges and can appear like in Figures 4 or 5, where the latter shows only one side of a parallel ridge.

Research into keel scours involves a variety of methods, including underwater surveys with sonar mapping like multibeam echosounders, autonomous underwater vehicles (AUVs), and satellite imaging for ice monitoring. These tools and techniques allow scientists to map and analyze the distribution, frequency, and characteristics of keel scours across different marine environments. This knowledge contributes to our understanding of the factors behind their formation, their temporal dynamics, and the environmental implications they may have (Shokr and Sinha, 2023).

2.4 Geophysical Research in the Beaufort Sea

2.4.1 Dynamics of Sediment Transport

To understand sediment transport processes in Arctic marine environments, researchers have conducted several studies on the Beaufort Sea. While Rearic et al., 1990 focused on sediment transport in the Alaskan Beaufort Shelf and found that ice-scour bulldozing played a significant role, Hill et al., 1991 showed that this phenomenon was specific to the region due to low fluvial sediment supply and limited open water conditions. On the Canadian Beaufort shelf, sediment transport by ice keel scour was insignificant compared to that from the Mackenzie River discharge. However, both studies highlighted the importance of ice scours as a critical indicator of regions experiencing more pronounced erosion and sediment transport. It is essential to study areas minimally affected by river transport. Therefore, this study focuses on Harrison Bay to further our understanding of ice keel scouring mechanisms and their impact on sediment transport in Arctic marine environments.

2.4.2 Characteristics and Implications of Knickpoint

According to the study of Barnes et al., 1987, the stamukhi zone appearing in the Beaufort Sea has a pronounced break in slope, referred to as the Knickpoint. This Knickpoint is at least 2 meters high and extends for over 150 kilometers in waters that are 18-23 meters deep. Linear shoals that are several meters high and about 100 meters in width can be found just inshore of the Knickpoint. The Knickpoint is a critical morphological transition associated with the inner boundary of the stamukhi zone and it can act as a barrier to the movement of ice keels, effectively stopping or altering their course. The Knickpoint was created by intense and repeated interactions between sea ice keels and the sea floor in the boundary of the stamukhi zone where interactions are heightened. This ongoing process results in the erosion of finer sediments and the accumulation of coarser materials. The presence of the Knickpoint significantly influences ice gouging rates across the stamukhi zone, and there is a noticeable increase in gouging intensity seaward of the Knickpoint. It is worth noting that while there has been some research conducted on the dynamics of ice keel scours in the Beaufort Sea, there still exists a significant research gap concerning the orientation of scours before the Knickpoint and how this may affect scour density. Addressing this gap in research could provide valuable insights into the interactions of scours and contribute to a more comprehensive understanding of the factors that influence the formation of shoals.

2.4.3 Ice Keel Scour Exploration

In a comprehensive study, Héquette et al., 1995 meticulously examined approximately 2200 ice scours that covered a 500 km area. The scours were classified into single and multiple types, with single scours accounting for the majority of the observations. The width of single scours ranged from 2 to 8 meters, with some extending over 40 meters. The depth of single scours was typically less than 60 centimeters, although a maximum depth of 2.2 meters was recorded. Single scours were mainly oriented East-West (96°), while multiple scours predominantly showed a Northwest-Southeast orientation (115°). This suggests that the dominant ice motion during scouring events is east or west, subparallel to bathymetric contours and coastline. In water depths of 12 to 18 meters, more than 75% of the seabed is typically reworked by ice scours. Scour dimensions increase with increasing water depth, with scours of all dimensions found in water depths of more than 10 meters.

2.5 Feature Extraction

2.5.1 Advancements in Automated Feature Extraction Techniques

Feature extraction techniques have become increasingly important in the field of geosciences. They enable researchers to analyze complex environmental data with unprecedented precision and speed. A recent article, Nellikkattil et al., 2024, highlights the crucial role of autonomous techniques in managing the exponential growth of climate data volume. This article describes a framework that combines topological methods, machine learning, and image-processing techniques for feature extraction from large climate datasets. Another example is the RivaMap library from Isikdogan et al., 2017, which is an automated river analysis and mapping engine designed to efficiently and accurately extract rivers from remotely sensed images on a large scale. RivaMap is a sophisticated model for river network extraction, facilitating the creation of large-scale maps of rivers and enabling the computation of extensive hydrography datasets. These papers demonstrate that efficient feature extraction significantly reduces the data volume required for storage and enhances computational efficiency in data analysis.

2.5.2 Modified Multiscale Singularity Index

The core metric utilized by RivaMap (as described in Isikdogan et al., 2017) is the modified multiscale Singularity Index (MMSI) ratio. This ratio is a dimensionless measure used in feature extraction methods for its ability to efficiently identify impulse singularities in signals of arbitrary dimensionality (Muralidhar et al., 2012). The MMSI formula is given by the equation 1:

$$MMSI = f_0 + f_1\theta + f_2\theta^2 + \sum_{i=1}^{n} \left[f_0^i \sigma(x_i, y_i) + f_1^i \theta_i \sigma(x_i, y_i) + f_2^i \theta_i^2 \sigma(x_i, y_i) \right] \tag{1}$$

where $f_0\ \theta\ \sigma(x, y)$, $f_1\ \theta\ \sigma(x, y)$ and $f_2\ \theta\ \sigma(x, y)$ are the responses to the zero, first and second order derivatives of Gaussians. σ and $\theta(x, y)$ specify the scale of the Gaussians and the direction of the derivatives, respectively. Using the second and third derivatives, it effectively identifies curvilinear-like structures while minimizing the responses to edges using the first derivative. As a result, it is less sensitive when the first derivative is prominent. To ensure its effectiveness, the singularity index is made invariant to local DC offsets through a process of local debiasing. This involves subtracting the local mean, which is computed using a large, unit area Gaussian filter. The singularity index is then computed at multiple scales, from finer to coarser, and the scale that yields the most significant scale-normalized index value is selected. The versatility of the Singularity Index ratio in extracting curvilinear-like structures across various data types makes it a suitable method for detecting ice keel scours in high-resolution Bathymetry measurements.

3 Study Area

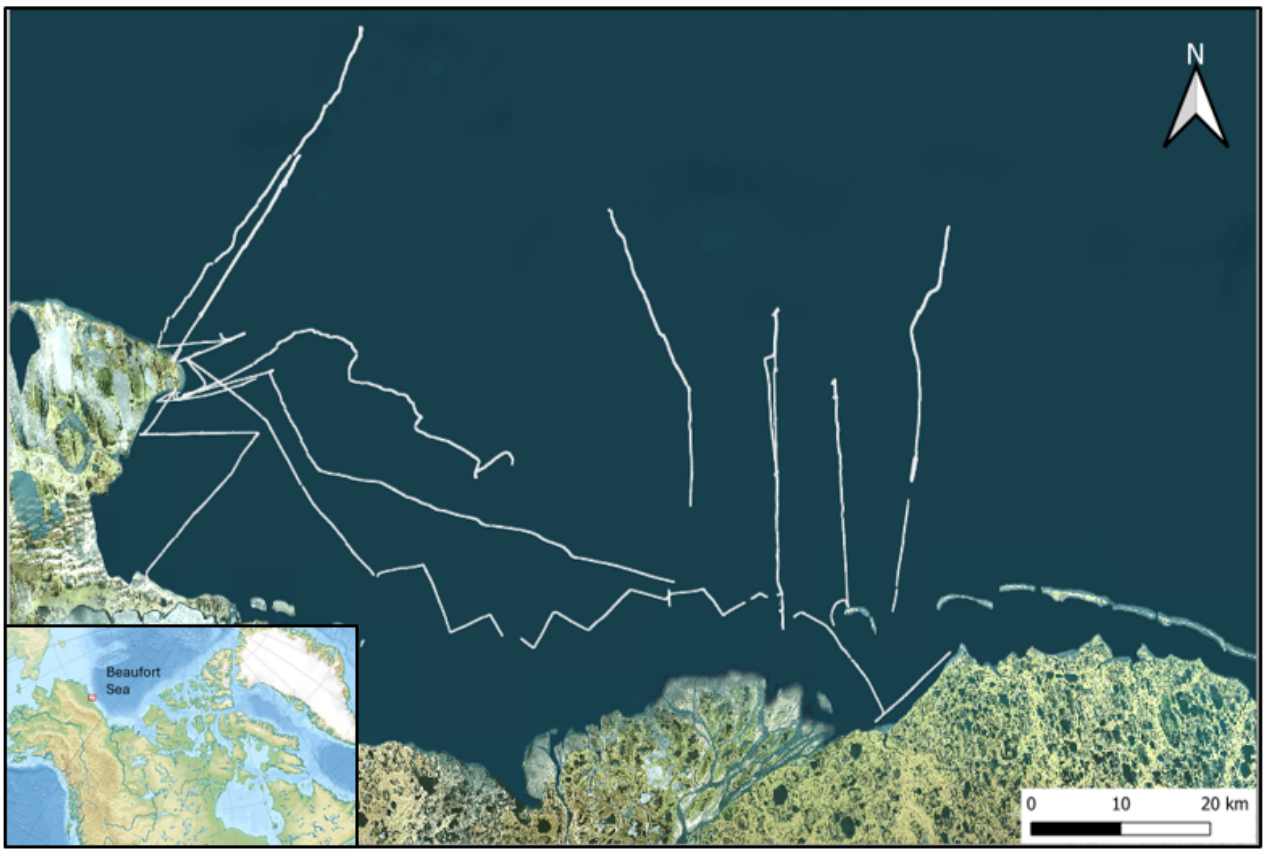

Figure 6: Study area along with a depiction of the measurements and its location in the Beaufort Sea.

The Beaufort Sea is a marginal sea of the Arctic Ocean, located north of the Northwest Territories, Yukon, and Alaska, and west of the Canadian Arctic Archipelago. It covers an area of 476,000 square kilometers and has an average depth of 1,004 meters, with its maximum depth reaching 4,683 meters Encyclopaedia Britannica, 2024. It is named after the British rear admiral Sir Francis Beaufort. The study area of this thesis can be seen in 6. Located north of Alaska in Harrison Bay, it is a part of the Beaufort Sea. The extensive bathymetric data that will be used will take place in these coordinates: 71°09′15″N to 70°26′16″N and 152°11′00″W to 149°46′49″W in front of the Colville River.

The study of Galley et al., 2013 displays how the Beaufort Sea is vital for exploring ecological and economic issues. The Beaufort Sea is important for offshore oil and gas exploration, particularly in the Prudhoe Bay oil field, which is adjacent to the area studied in this thesis. Knowing the concentration of sea ice is crucial for the success of oil operations, but the region's ice gouging presents significant challenges to the stability of sub-sea pipelines.

4 Methods

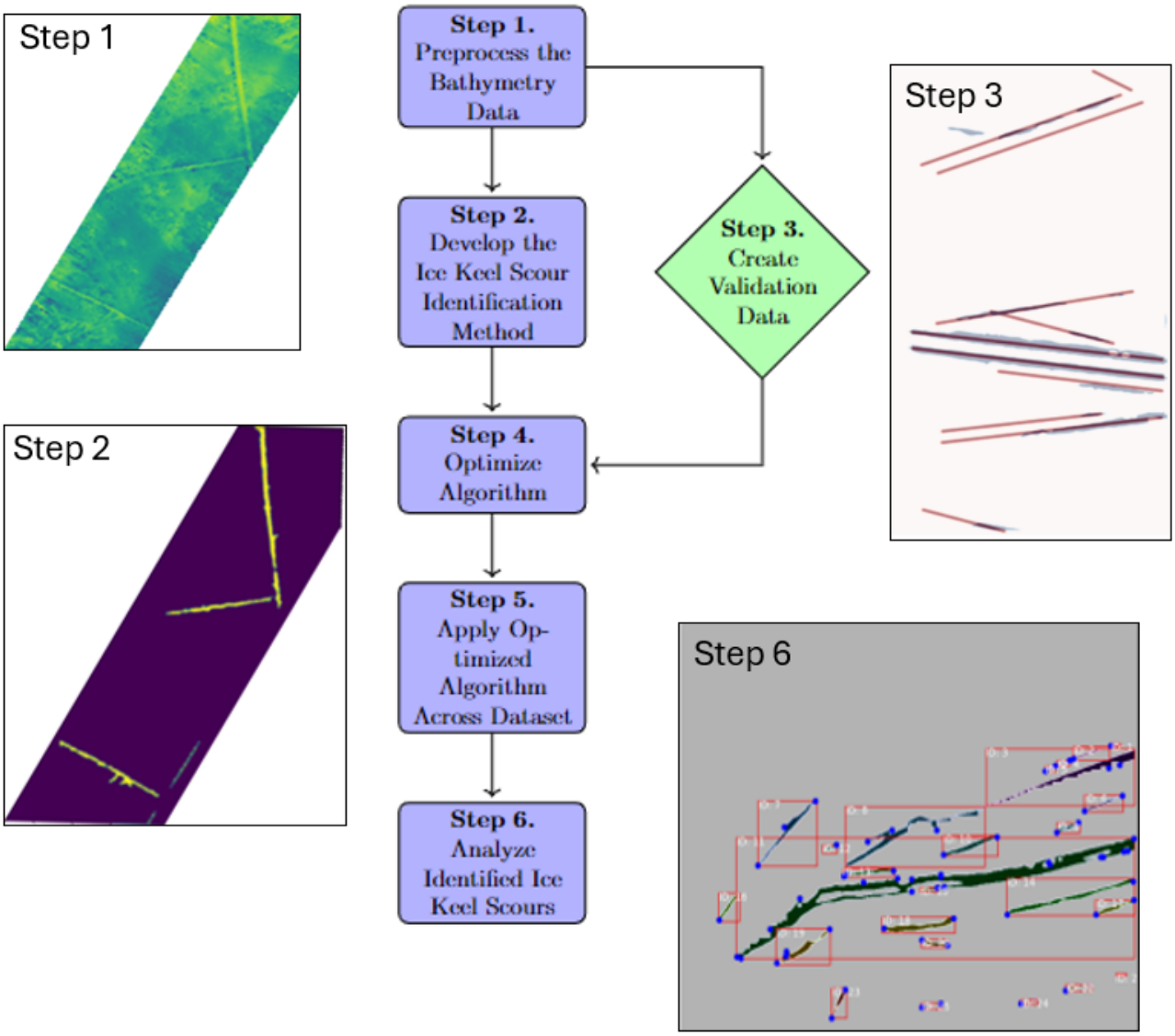

Figure 7: Depiction of this study's methodology flowchart and a few outcomes from selected steps.

4.1 Bathymetric Data Received From Beaufort Sea Surveys

This thesis utilizes extensive bathymetric data derived from the Beaufort Sea, collected during a survey aboard the R/V Ukpik in the summers of 2021 and 2022, led by Chief Scientist Emily Eidam. Advanced multibeam sonar systems were employed to map the seabed depth and topography. The survey resulted in the acquisition of over 100 kilometers of multibeam survey tracks at depths lower than 20 meters offshore of the Colville Delta and Cape Halkett. The data was thoroughly processed for accuracy and reliability.

4.2 Step 1. Preprocess of Bathymetry Data

In order to provide a foundational dataset for the development and testing of the automated ice keel scour identification algorithm, the spatial data was divided into discrete tiles, each measuring up to 200x200 meters and a pixel value of 0.08 meters. These tiles were generated from the measurements, starting from minimum easting and northing values, covering the entire area of each data file. One such tile showcasing visible ice keel scours is depicted in Figure 8. It should be noted that despite being uniform in size, the areas of measurements within each tile varied. This approach allowed for more manageable data sections, facilitating the algorithm's development. Each tile was assigned a unique number and aligned with the Beaufort Sea coordinates to pinpoint any data discrepancies and contextualize the scours within the larger geographical context. This process provided a clearer understanding of the seabed's structure, laying the groundwork for subsequent research.

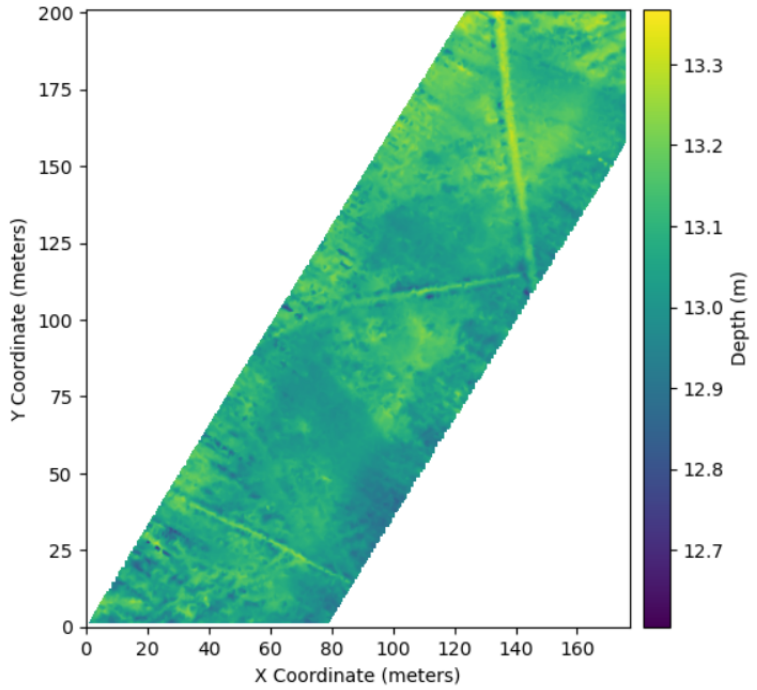

Figure 8: Resulting bathymetric tile from Step 1, showing visible ice keel scours. The color scale indicates depth, with variations that highlight underwater scour features.

4.3 Step 2. Developing the Ice Keel Scour Identification Method

The critical step in developing an automated algorithm for identifying ice keel scour in this thesis is using the Modified Multiscale Singularity Index (MMSI). This is because it can adjust the depth value of the measurements. Typically, the depth difference between furrows and the surrounding area is minimal, with only a few centimeters difference, but the MMSI assigns a value based on curvilinearity. To apply the MMSI function, the image must first be normalized by scaling pixel values to a range between 0 and 1. Adjusting the minScale (minimum Scale) and nrScale (number of Scales) parameters is also essential to achieving optimal results. These parameters determine the smallest scale at which the singularity index response is computed and the number of scales the analysis is conducted (Isikdogan et al., 2017). Finding the optimal values for the singularity index is crucial as the resulting response varies with pixel size and image dimensions.

A series of image processing techniques are employed to enhance the singularity index response and emphasize curvilinear features. The initial thresholding transformes the image into a binary format, isolating high-response regions. A secondary threshold then eliminates regions smaller than a predefined pixel count, followed by a final threshold that isolates and retains only elongated areas within these high-response regions. In the image shown in Figure 9, the right panel depicts the output of the Ice keel scour identification algorithm. The resulting binary image highlights the identified scours in yellow color. The threshold values used for the algorithm are visible in Table 1.

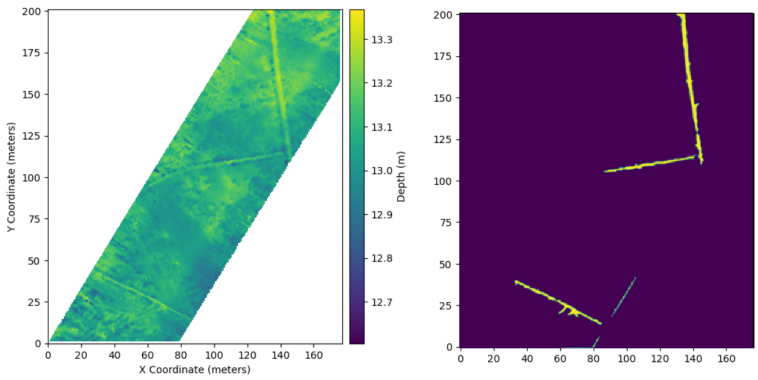

Figure 9: Resulting binary image of step 2. The right panel is the binary image with scours highlighted in yellow and the left panel is the original image also shown in Figure 8

4.4 Step 3. Creating Validation Data

In order to validate and optimize the algorithm, a total of 67 images were employed. These images were classified and systematically categorized into four distinct levels based on the prominence of scour features such as ridges and depth variations. This categorization aimed to ensure that the ground truth data covered a wide range of scour formations, allowing the algorithm to be tested against a diverse set of examples rather than a uniform dataset. The ground truth data comprised rasterized images of manually drawn center lines of the scours visible in the processed multi-beam bathymetric data from the Beaufort Sea. The center lines were expanded to a width of 1.36 meters. Overall, 423 scours were rasterized for this process. Figure 10 showcases an example from the validation process, displaying the processed tile derived from the bathymetry measurements alongside the corresponding rasterized and algorithmically identified scour. With red are the rasterized scours and the blue areas are the algorithmically identified scours.

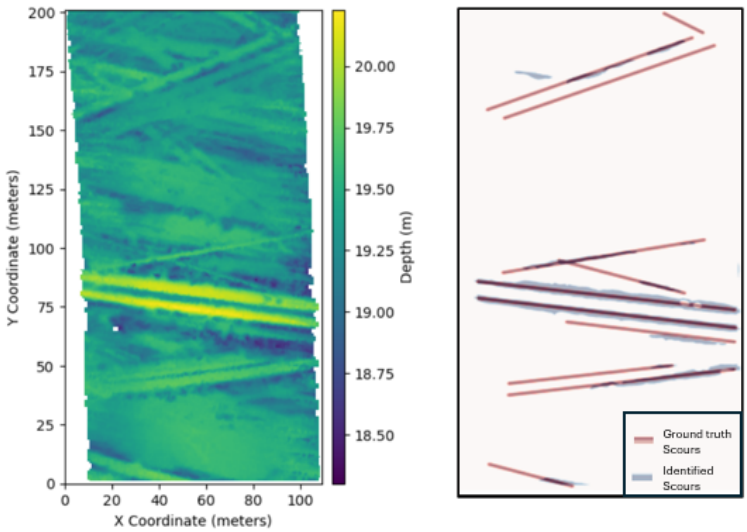

Figure 10: Example of the validation process. The left panel is the original image used to create ground truth scours, and the right panel shows the rasterized ground truth scours along with the identified scours from the algorithm.

4.5 Step 4. Optimizing the Identification Algorithm

Using the pixels of ground truth data along with the pixels from the identification algorithm provides the four fundamental elements used for evaluating the performance of the algorithm.

- True Positives (TP): Pixels correctly predicted as ice keel scours.
- False Positives (FP): Pixels incorrectly predicted as ice keel scours.
- True Negatives (TN): Pixels correctly predicted as non-ice keel scours.
- False Negatives (FN): Pixels incorrectly predicted as non-ice keel scours.

The foundational elements outlined above serve as the basis for calculating the performance metrics presented in Table 1. These derived metrics provide a comprehensive evaluation of the algorithm's efficacy, highlighting its successes and pinpointing opportunities for refinement.

- Sensitivity (also known as Recall or True Positive Rate) is TP/(TP+FN) and measures the percentage of correctly identified positive instances relative to the total number of actual positives.
- Precision is TP/(TP+FP) and indicates the percentage of positive identifications that were actually correct.
- Specificity is TN/(TN+FP) and measures the proportion of actual negatives that were correctly identified.

minScale	nrScales	minArea	Threshold (SI)	E-Filter	Sensitivity (%)	Precision (%)	Specificity (%)
5	5	1000	0.9	5	47.56	21.15	96.25
5	5	700	0.97	7	23.27	25.07	98.53
5	5	200	0.94	6.5	35.17	16.53	96.25
5	5	500	0.95	7	34.34	28.71	98.20
5	5	245	0.945	6.5	36.11	31.16	98.31
1.25	10	245	0.945	6	33.58	24.51	97.81
3.25	5	245	0.945	6	36.82	33.37	98.44

Table 1: Performance metrics of the algorithm evaluated across various parameter settings.

The validation process for the identification algorithm was not a one-off event but an iterative one. Table 1 displays examples of the algorithm's process with all five parameters, which were constantly adjusted based on the confusion matrix results. The grid search method was employed for hyperparameter tuning, to improve the algorithm's precision. This process involved testing numerous combinations of the five hyperparameters shown in Table 1 across predefined values ranges to identify the algorithm's optimal configuration. The last set of parameters seen in Table 1 is the final set of hyperparameters used and returned in the most optimized form of the algorithm.

The F1 score was used to assess the performance of each parameter set, as it provides a balanced treatment of precision and recall, which is particularly important in contexts of data imbalance. As noted in Wardhani et al., 2019, this metric accurately depicts a model's predictive accuracy more than traditional metrics. The F1 score's ability to simultaneously consider false positives and false negatives ensured a more comprehensive and reliable evaluation of the model's performance.

4.6 Step 5. Apply Optimised Algorithm Across Dataset

Following the optimization of the ice keel scour identifying code, the refined algorithm was applied across all Bathymetric Data received. This process generated 5033 tiles of seabed images, each highlighting the identified scours as binary images. The area of measurement covers about 45 square kilometers and reaches depths of up to 28 meters.

4.7 Step 6. Analyse Identified Ice Keel Scours

4.7.1 Scour Pattern Characterization and Measurement Extraction

The final phase of this study involves extracting key measurements from the identified ice keel scours. This process uses an automated extraction of key measurements from the resulting binary scour images while ensuring the integrity and traceability of the associated metadata for each scour pattern. A segmentation of the scours is done by labeling them to identify individual scour patterns, and calculating each one's size and orientation. Specifically, the process skeletonizes the scour patterns to determine their structural endpoints, enabling the calculation of their orientation in degrees and the estimation of their average width based on the area and length of each scour. Figure 11 illustrates the identified scours with their respective structural endpoints. The Right Panel showcases the identified scours positioning with ID tags and overlaid red squares. These squares represent the bounding boxes used to infer the length and orientation of the scours, with the diagonal serving as a proxy for maximum scour extent.

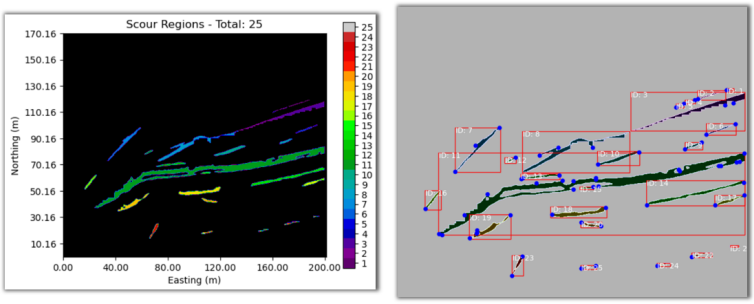

Figure 11: Visualizing Scour Patterns: A Multicolored Map and Dimensional Analysis. The left panel displays a vivid map with 25 individual scour regions, each color-coded for easy distinction. The right panel showcases a detailed analysis done for each scour region.

The information, considered as key measurements, is meticulously recorded in a metadata structure for each identified scour, capturing essential details like endpoints and angular orientation. This information, which includes depth, coordinates, widths, and orientation, can be essential for better understanding the dynamics of ice-keel scour formation and its interaction with the seabed. This information is then methodically stored, guaranteeing that each data point is preserved alongside its corresponding metadata for subsequent analysis and research.

4.7.2 Tile-Based Analysis of Scour Data

This thesis will take single measurements per tile to analyze ice keel scours. This will allow us to derive specific scour information per tile and make an analysis of the scour patterns identified in the Harrison Bay study area. We will record the average depth and center coordinates for each of the 5033 tiles used in this thesis. Additionally, we will record the maximum widths identified per tile to analyze the width of the ice keel scours. The maximum widths are taken for they represent the most well-defined scours identified in each tile. To assess scour density, we will measure the percentage of scour areas per tile area and the number of scours per tile. However, it is essential to note that the tiles are all different sizes, so there may be some discrepancies. Therefore, we should focus on the correlation between values rather than the values themselves. Lastly, the most prominent orientation of scours will be recorded per tile.

5 Results

5.1 Preliminary Analysis Overview

Looking at the average depths of the tiles presented in Figure 12, we can conclude that most measurements are in depths up to 20 meters. Furthermore, at the 20-meter mark, there is a pronounced decrease, with the number of measurements from 20 to 28 being only a small fraction of the whole.

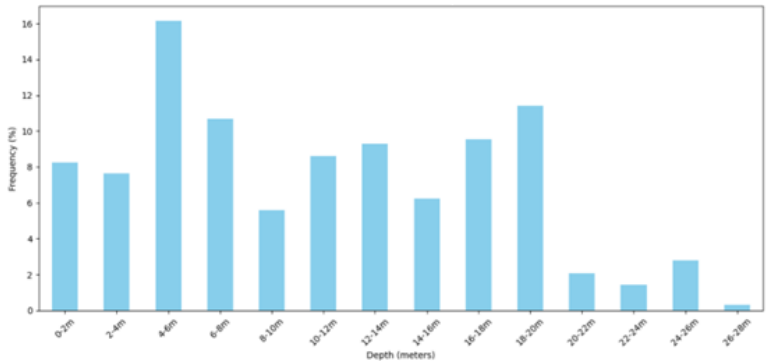

Figure 12: Distribution of tile depth where the x-axis shows the average depth calculated for each tile and the y-axis the frequency of these depths in percentages

The frequency of maximum scour widths per tile observed in this study is presented in Figure 13. The histogram shows that the distribution of scour widths is right-skewed, with a noticeable peak in the range of 1.0-3.0 meters, which indicates that this is the most common width interval. Scour widths beyond 5 meters are sparse, while widths up to 12 meters have been identified.

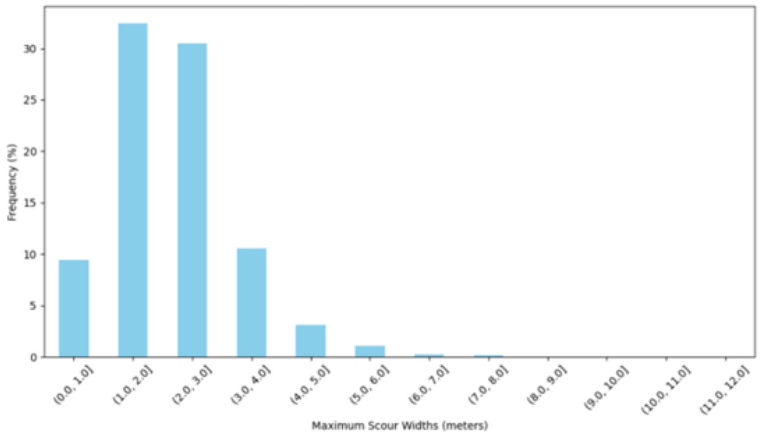

Figure 13: Histogram of maximum scour widths calculated for each tile [, with the x-axis showing the meters and the y-axis showing the frequencies of those widths in percentage.]

Figure 14 demonstrates the number of scours per tile and shows an exponential decay. The highest frequency of scours is in the first 2 bars, with values from 0 to 6 scours. The frequency decreases rapidly at first and then levels off, with values reaching up to 54 scours in a tile.

A similar declining trend is also visible in the histogram of the scour percentages per tile (Figure 15). Here the highest frequency is for tiles that had an area of less than 1 percent of identified scours. The highest percentage of scours in a tile is 5.5 percent. Even though the similarity in these two graphs is high, the outliers in the second graph are high in number. The 5.5 percent represents a very small tile with only one scour at a depth of 6 meters. This outlier represents many of the tiles analyzed for scour percentage. For this reason, the scour area percentages calculated do not indicate scour density. The number of scours in a tile, however, indicates how many parts in a tile have a curvilinear structure and, therefore, the density of scours in that area of tiles. Due to the different tile sizes, the number of scours will vary greatly. However, tiles with a high number of scours will still represent dense scour areas.

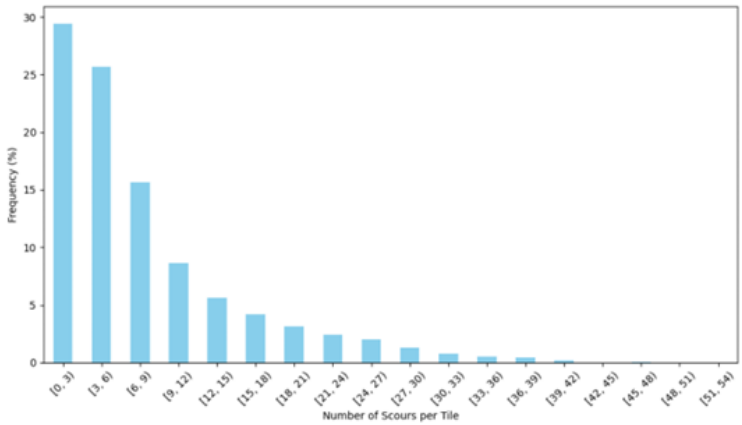

Figure 14: Histogram displaying the number of scours per tile. The x-axis represents the bins of the scour counts and the y-axis displays the corresponding frequency of these occurrences.

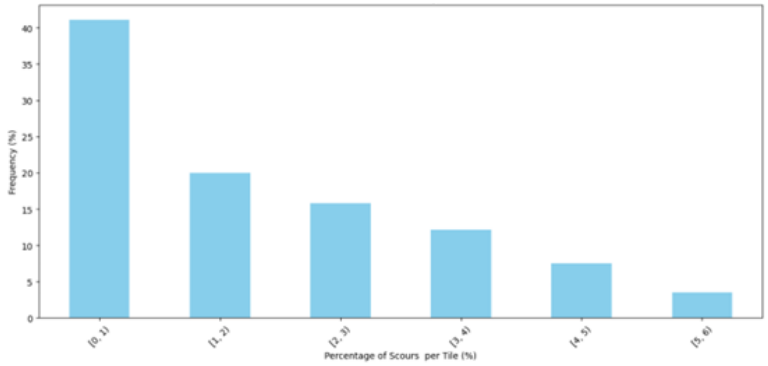

Figure 15: Histogram of scour percentages per tile.

In this study, scour orientations are measured from North (0 degrees) to South (180 degrees) in a clockwise direction due to the inability to ascertain the exact direction of sea ice movement. As a result, the orientations indicate the angles at which the ice keels moved, using a 0 to 180-degree scale, rather than the specific direction of the ice keels. The highest frequency, between 80 and 100 degrees seen in Figure 16, indicates alignment with the eastern direction.

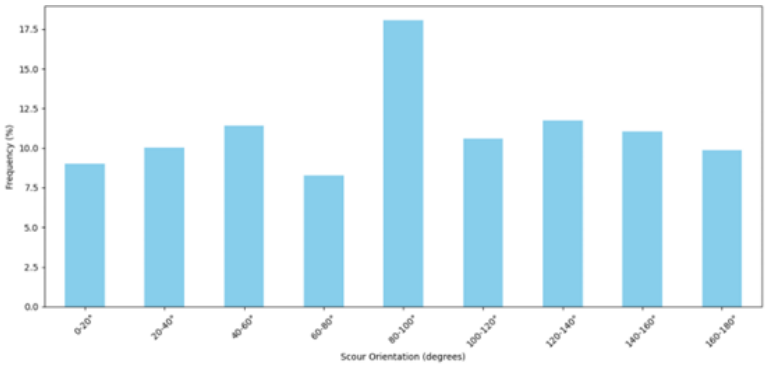

Figure 16: Orientations analyzed per tile. The x-axis displays the slope orientations in degrees starting from North and the y-axis represents the percentage of those slopes.

5.2 Scour Width Variation by Depth

The scour width does not seem to be significantly affected by depth, as indicated by Figure 17. The trendline seen in Figure 17 shows a small slope indicating a slight positive correlation between depth and scour width. The slope suggests that the width increases by 44% at the highest depths, implying that deep parts of the sea have wider scours. However, it is essential to note that depth alone has limited explanatory power. This is

supported by an R-squared value of only 0.04, meaning that depth accounts for just 4 percent of the variation in scour width. However, the P-value is highly significant and cannot be overlooked. This underscores the statistical relevance of the relationship and suggests that while not the dominant factor, the depth of a tile does influence the maximum width of scours to some extent (Kutner et al., 2005).

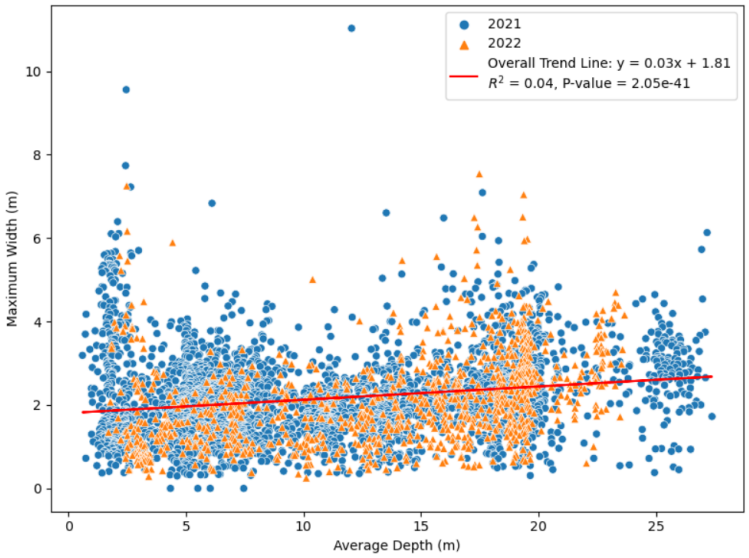

Figure 17: Scatter plot showing the relationship between each tile's average depth (x-axis) and its maximum scour width (y-axis) identified, with a trendline highlighting the overall measurement trend.

5.3 Scour Density Variation by Depth

Increasing depth is positively correlated with a higher concentration of scours, as depicted in Figure 18. The trendline's upward slope supports this conclusion. Specifically, the trendline shows a significant 580% increase from the starting point to the last point, indicating a substantial change in scour density across the range of depths studied. However, the coefficient of determination indicates that only about 21% of the variation in scour density can be attributed to changes in depth. Nevertheless, the low P-value emphasizes the statistical significance of depth's influence on scour density. This pattern is illustrated by the fact that at deeper depths, the tiles have a higher number of scours, with more than 60% of tiles having more than 10 scours. On the other hand, at shallower depths, the percentage of tiles with more than 10 scours is less than 10%. These findings confirm the critical role of depth in determining the distribution and density of ice keel scours, supporting the hypothesis that depth is a crucial factor in the spatial variability of scour occurrences.

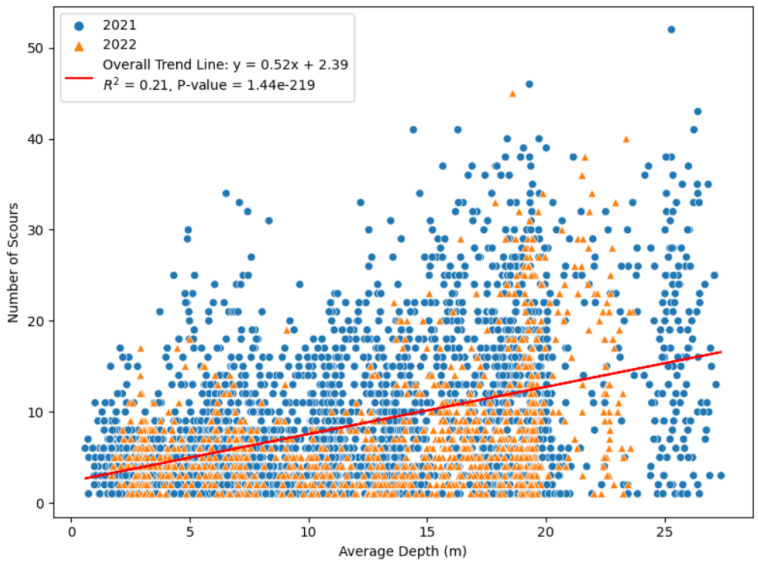

Figure 18: Scatter plot of the Number of scours identified against the average depth for a selected tile. The trendline represents the overall measurement trend

5.4 Spatial Distribution and Orientation of Ice Keel Scours

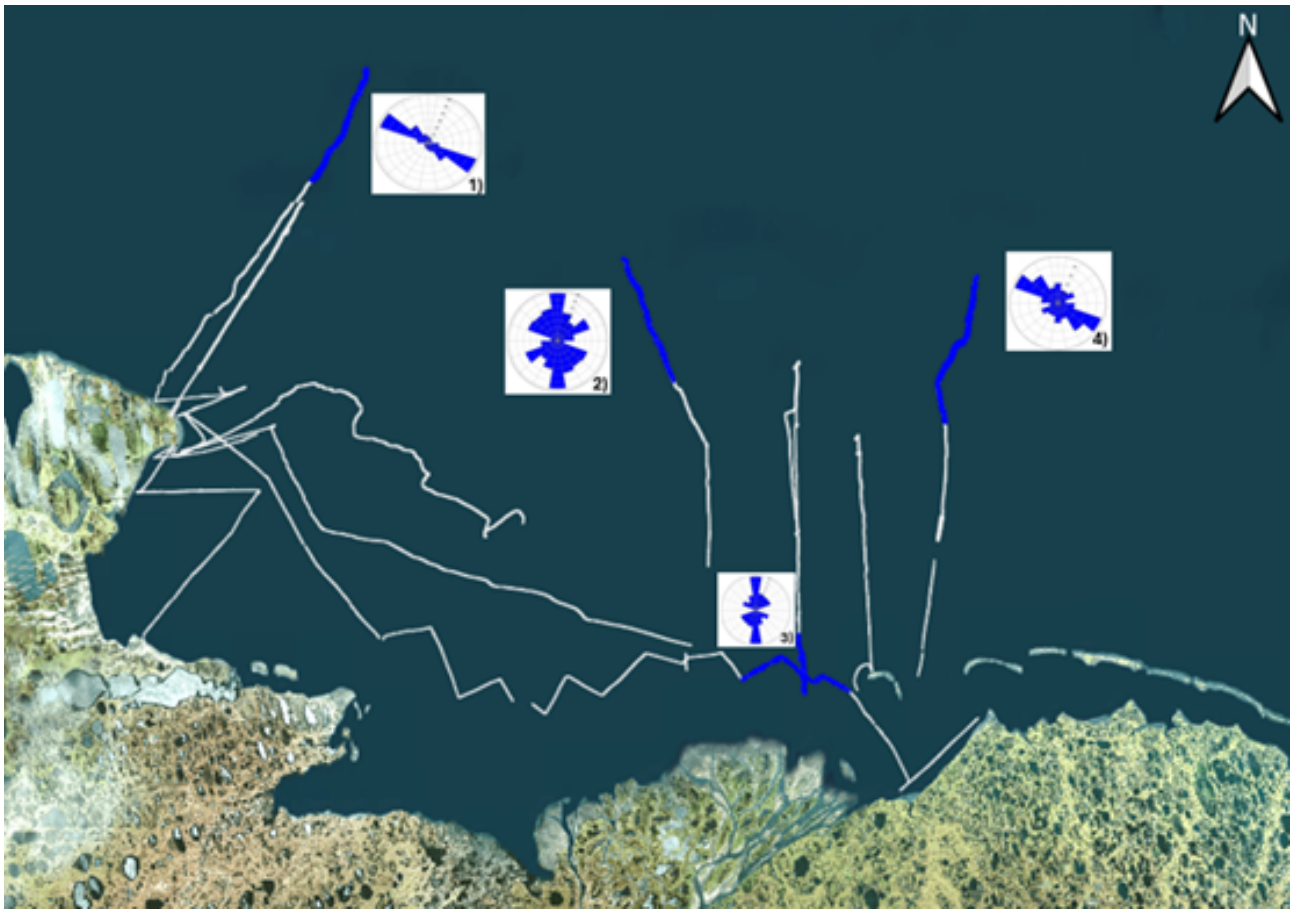

Figure 19: Spatial distribution of measurements across the study area, with inset polar plots highlighting scour orientation from four areas of interest.

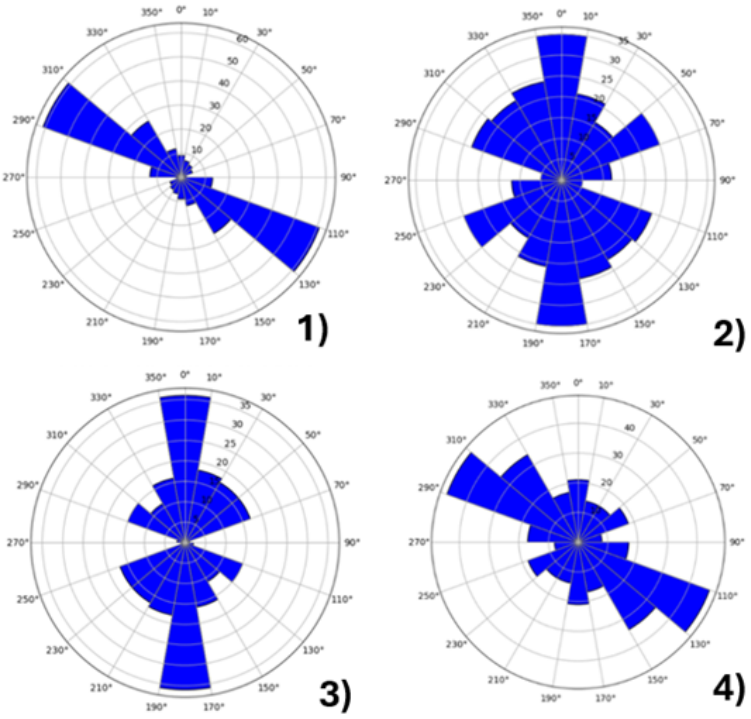

Figure 20: Polar histograms representing scour orientation in the four areas of interest.

In Figure 19, circular bar charts are presented, showcasing the orientation of scours from measurements of specific areas. Area 1, highlighted for better visualization in Figure 20, reveals a strong concentration of orientation towards 120 and 300 degrees, with minimal variability. Based on this data, we can infer that most scours are aligned in a southeasterly direction, likely influenced by consistent environmental conditions governing the movement of sea ice in this particular sea region.

The circular bar chart depicting the scour orientations in Area 2 reveals a range of patterns, with a marked prevalence of the north-to-south axis at 0 degrees. While the data displays a diversity of influences contributing to the formation of scours, the trend towards a north-south trajectory remains distinct.

Area 3 is located in close proximity to the Colville River, as indicated in Figure 20. The polar histogram displays minimal directional variation with a distinct trend along the north-to-south axis. This predominant orientation highlights the crucial role of hydrological influences in the formation of directional scours in this area.

Area 4 shares similarities with Area 1 in terms of its deeper waters and dominant scour orientation along the 120 and 300-degree directions. However, there is a slightly greater degree of directional variation present in this area, which suggests the potential influence of a wider range of factors in this location.

6 Discussion

6.1 Objectives and Successes of the Study

This study aimed to leverage advancements in computational research methods to develop an algorithm for the automated identification of ice keel scours and conduct an automated analysis of the identified scours. Large bathymetric datasets were processed, offering a faster and more accurate alternative to traditional manual inspection and analysis methods used in previous research studies such as Héquette et al., 1995 and Blasco et al., 1998. More specifically, the method used in this study can show the accuracy of the measurements compared to manual methods that rely on the subjective interpretation of the examiner. The algorithm developed shows a precision rate of 33% across all classes of digitized scours. This low precision points to the fact that While the algorithm is not always successful in identifying complex or altered scours, it is effective in identifying newer scours that still possess side ridges and distinct furrows without heavy infilling. This can be seen in Figure 10. In addition, the automated analysis process enabled extracting and recording critical measurements for each identified scour, streamlining comparison with previous studies. Instead of using each individual scour for analysis, this study relied on the tiles used for scour identification. While this approach offered a pragmatic method to derive preliminary insights into scour characteristics and patterns, it is important to note that it had some limitations. However, given the time constraints of this study, this simplified method provided a reasonable basis for analysis. These deviations underscore the need for further research to refine the algorithm's accuracy and analytical methodology.

6.2 Findings Comparement to Prior Studies

6.2.1 Ice Keel Scour widths

Based on my analysis of scour widths, I have discovered measurements that are notably smaller than those reported in previous studies such as Héquette et al., 1995 and Blasco et al., 1998. Interestingly, the scour analysis in this study is highly comparable to that conducted by Héquette et al., 1995, which focused on scours up to 20 meters deep in the same sea of Beaufort as the measurements used in this study. Despite this similarity in depth range, there are significant differences in the measured scour width. These dissimilarities may arise from discrepancies in the ice keel scour identification algorithm or the methodology of width analysis. Furthermore, the discrepancies may be attributed to variations in environmental factors between the current study area and Héquette's study area. In Héquette's study, the focus was on the Mackenzie River estuary, which led to increased sea ice movement and therefore increased scouring.

According to the findings of Héquette et al., 1995, the range in width measurements is five times wider than the one obtained in this study. However, the highest frequencies are found in similar widths, with Héquette's study showing a range from 2 to 6 meters and this study revealing a range from 1 to 3 meters. Additionally, the distribution pattern of widths, characterized by an initial increase followed by a long tail, remains consistent across both studies. This pattern suggests a fundamental similarity in scour formation processes despite the variance in measured widths.

Furthermore, the minimal increase in width with depth observed in my data, supported by a low coefficient of determination, suggests a negligible correlation within the depth range primarily studied. Although studies have shown that greater widths are visible in deeper waters, those studies point to depths greater than the Knickpoint, which is at a depth of between 18 to 23 in the Beaufort Sea. The presence of the Knickpoint is suggested by the sudden decrease in data, seen in Figure 12. This phenomenon was also observed in the Bathymetry measurements, where the depths in certain regions were shallower than anticipated due to the presence of shoals. Following the Knickpoint, there was a marked increase in depths. This research, therefore, is primarily conducted behind the Knickpoint, and the increase in width may not be comparable to those studies.

6.2.2 Ice Keel Scour Density

According to this analysis, the density of scours tends to increase with depth. However, unlike the exponential increase observed by Héquette et al., 1995 beyond 10 meters depth, this study indicates a linear rise in density, as shown in figure 18. It is worth noting that the break in slope that Héquette discovered in Tuktoyaktuk Bay is not found in this region. This could be attributed to the fact that the environmental factors affecting shallow waters in this area are less significant than those in Tuktoyaktuk, where the Mackenzie River plays a role. As a result, the increase in scour density is more linear than exponential.

6.2.3 Orientation of Ice Keel Scours

As described in literature such as Héquette et al., 1995 and Blasco et al., 1998, the orientation predominantly follows an east-southeast direction. Both Hequette's and this study indicate that there is a significant orientation at 100 degrees. On the other hand, Blasco's study found that most orientations were at 120 degrees, which also aligns well with this study. My analysis shows that closer to the coastline and behind the Knickpoint, scours exhibit greater variation in orientation, with a prominent north orientation, while in front of the Colville River estuary, the orientation is mainly toward seawater (North). However, in deeper waters, the ocean circulation causes the east-southerly direction seen in all three studies, presumably due to the Beaufort Sea Gyre. The orientation found in waters at and after the Knickpoint is primarily at 120 degrees, similar to the scours found in Blasco's study, which also had measurements deeper than the Knickpoint.

6.3 limitations and Possible Improvements

6.3.1 Automated Identification Algorithm

The automated algorithm developed for ice keel scour identification has shown promising results, but it also has some limitations that need to be addressed. One of the main challenges is the difficulty of observing ice keel scours due to the majority being reworked and the furrows being refilled. Moreover, the newer scours interact and alter the ridges of prior scours, creating interconnected structures that are hard to identify. To overcome these limitations, further work is needed in the optimization phase. The work of Isikdogan et al., 2017 validated their singularity index by drawing orthogonal lines in the river orientations at certain centerlines. This study did something similar by expanding the width of centerlines in a variety of studies. However, this was only one way Isikdogan et al., 2017 validated and optimized their automated identification method. They compared the identified width estimates with in-situ measurements from the Water Survey of Canada (WSC) and the NARWidth dataset. This comparison involved 902 out of the 1049 in-situ measurements that were automatically detected by their algorithm. This means that the most essential part of the identification code, which is to identify the entire extent of the river successfully, had extensive ground truth data to validate and optimize it. By optimizing and validating the algorithm primarily for newer and more distinct scours, it is expected that the precision values will be improved, leading to a more accurate and reliable identification of ice keel scours.

6.3.2 Automated Ice Keel Scour Analysis

Improvements can be made to the automated analysis of identified ice keel scours. Rather than creating small patches of measurements that produce outliers, scour identification can be performed in larger images. Additionally, analyzing each identified scour individually rather than as part of a whole patch requires digitizing and saving each scour while geocoding it for assessment as part of the entire measurement area. To achieve this, an algorithm must correlate scours at the edges of each parchment with those on the next, allowing for identifying scours as a continuation rather than separate entities. Results from this refined analysis will bring even more scour characteristics, including the depth and number of scours per square kilometer. These improvements will enhance the reliability of scour dimension assessments, contributing to a more nuanced understanding of scour morphology and its influencing factors across various depths and environmental conditions.

7 Conclusion and Future Work

In conclusion, using bathymetric data and the Modified Multiscale Singularity Index, this study was able to identify and analyze ice keel scours in the Beaufort Sea. The results showed variations in scour width and density with depth, as well as a spatial distribution and orientation pattern of the scours. While the proposed automated ice keel scour extraction method successfully achieved its objectives, there is still room for improvement in future studies. To enhance the accuracy of the automated identification algorithm and analysis, it would be beneficial to optimize the algorithm using a significant amount of ground truth data and accurately identifying the width of the scours. Additionally, conducting an analysis of the waters after the knickpoint and comparing it to the data collected before the knickpoint could provide valuable insights. Overall, this study offers a thorough analysis of ice keel scours by utilizing bathymetric measurements from the Beaufort Sea. The findings can be used to enhance future research and improve our knowledge of sediment transport dynamics and the characteristics of ice keel scours in the Arctic Ocean.

8 Acknowledgements

This research was funded by the National Science Foundation (1913195). First and foremost, I want to express my gratitude towards my supervisors, Jaap Nienhuis and Menno Straatsma, for their invaluable guidance, patience, and constructive feedback throughout my research. Additionally, I am Thankful for the data collection efforts led by Emily Eidam, along with the team of Dan Duncan, Jaap Nienhuis, Nick Brilli, Nina Stark, Josephine Hall, and Caroline Cooper.

References

Barnes, P. W., Asbury, J. L., Rearic, D. M., & Ross, C. R. (1987). Ice erosion of a sea-floor knickpoint at the inner edge of the stamukhi zone, beaufort sea, alaska. *Marine geology*, *76*, 207–222.

Blasco, S., Shearer, J., & Myers, R. (1998). Seabed scouring by sea-ice: Scouring process and impact rates [Canadian Beaufort Shelf]. *Proceedings of Ice Scour and Arctic Marine Pipelines Workshop, 13th International Symposium on Okhotsk Sea and Sea Ice*, 53–58.

Dieckmann, G. (2003). *Sea ice: An introduction to its physics, chemistry, biology, and geology.*

Eicken, H., Gradinger, R., Gaylord, A., Mahoney, A., Rigor, I., & Melling, H. (2005). Sediment transport by sea ice in the chukchi and beaufort seas: Increasing importance due to changing ice conditions? *Deep Sea Research Part II: Topical Studies in Oceanography*, *52*(24-26), 3281–3302.

Encyclopaedia Britannica. (2024). Beaufort sea – arctic ocean, wildlife oil exploration. https://www.britannica.com/place/Beaufort-Sea%7D%7D

Galley, R. J., Else, B., Prinsenberg, S., Babb, D., & Barber, D. (2013). Summer sea ice concentration, motion, and thickness near areas of proposed offshore oil and gas development in the canadian beaufort sea—2009. *Arctic*, 105–116.

Héquette, A., Desrosiers, M., & Barnes, P. W. (1995). Sea ice scouring on the inner shelf of the southeastern canadian beaufort sea. *Marine Geology*, *128*(3-4), 201–219.

Hill, P. R., Blasco, S. M., Harper, J. R., & Fissel, D. B. (1991). Sedimentation on the canadian beaufort shelf. *Continental Shelf Research*, *11*(8-10), 821–842.

Isikdogan, F., Bovik, A., & Passalacqua, P. (2017). Rivamap: An automated river analysis and mapping engine. *Remote Sensing of Environment*, *202*, 88–97.

Kutner, M. H., Nachtsheim, C. J., Neter, J., & Li, W. (2005). *Applied linear statistical models.* McGraw-hill.

Lusilier. (2023a). Seabed scouring by ice [Accessed: 29 March 2024. Available under CC BY-SA 4.0. Contributed by Lusilier to Wikipedia.].

Lusilier. (2023b). Stamukha drawing [Accessed: 29 March 2024. Available under CC BY-SA 4.0. Contributed by Lusilier to Wikipedia.].

Muralidhar, G. S., Bovik, A. C., & Markey, M. K. (2012). A steerable, multiscale singularity index. *IEEE Signal Processing Letters*, *20*(1), 7–10.

National Snow and Ice Data Center / Arctic Monitoring and Assessment Programme. (2021). Image on arctic currents [Accessed: [your access date]. Image credit: NSIDC/AMAP, https://nsidc.org/learn].

Nellikkattil, A. B., Lemmon, D., O'Brien, T. A., Lee, J.-Y., & Chu, J.-E. (2024). Scalable feature extraction and tracking (scafet): A general framework for feature extraction from large climate data sets. *Geoscientific Model Development*, *17*(1), 301–320.

Rearic, D. M., Barnes, P. W., & Reimnitz, E. (1990). Bulldozing and resuspension of shallow-shelf sediment by ice keels: Implications for arctic sediment transport trajectories. *Marine geology*, *91*(1-2), 133–147.

Reimnitz, E., Toimil, L., & Barnes, P. (1978). Arctic continental shelf morphology related to sea-ice zonation, beaufort sea, alaska. *Marine Geology*, *28*(3-4), 179–210.

Shokr, M., & Sinha, N. K. (2023). *Sea ice: Physics and remote sensing.* John Wiley & Sons.

Szafarczyk, A., & Toś, C. (2022). The use of green laser in lidar bathymetry: State of the art and recent advancements. *Sensors*, *23*(1), 292.

Thomas, D. N. (2017). *Sea ice.* John Wiley & Sons.

Wang, M., & Overland, J. E. (2015). Projected future duration of the sea-ice-free season in the alaskan arctic. *Progress in Oceanography*, *136*, 50–59.

Wardhani, N. W. S., Rochayani, M. Y., Iriany, A., Sulistyono, A. D., & Lestantyo, P. (2019). Cross-validation metrics for evaluating classification performance on imbalanced data. *2019 international conference on computer, control, informatics and its applications (IC3INA)*, 14–18.

Weatherall, P., Marks, K. M., Jakobsson, M., Schmitt, T., Tani, S., Arndt, J. E., Rovere, M., Chayes, D., Ferrini, V., & Wigley, R. (2015). A new digital bathymetric model of the world's oceans. *Earth and space Science*, *2*(8), 331–345.

Zhang, Q. R. (1992). Geological models of ice keel scours, with an early sinian example. *Precambrian research*, *59*(3-4), 315–323.

9 Appendix I

During the analysis certain discrepancies within the dataset became evident, specifically in regions with low-depth profiles. These anomalies were characterized by areas exhibiting high depths at their centers and linearly low depths at their peripheries. Such irregularities led to the misclassification of large scours by the automated identification algorithm due to the algorithm's interpretation of these depth variations as indicative of scour presence. After identifying them and ensuring they are falsely described scours, the 18 most extreme Measurements (14 from 2021 and 4 from 2022) are considered outliers and excluded from the dataset. This means that from the 3350 tiles that have more than zero scours identified, 18 will be excluded. Figure 21 below shows an example of such an outlier.

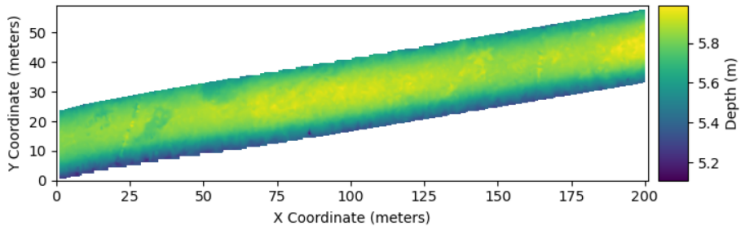

Figure 21: Example of an outlier tile that shows higher depths in the center and increased height on the sides creating a false scour: Tile with the highest maximum width of scour identified in measurements of 2022.